



1                   **Central Arctic Ocean paleoceanography from ~50 ka to present,**  
2                   **on the basis of ostracode faunal assemblages from SWERUS 2014**  
3                   **expedition**

4  
5 Laura Gemery<sup>1</sup>, Thomas M. Cronin<sup>1</sup>, Robert K. Poirier<sup>1&2</sup>, Christof Pearce<sup>3,4</sup>, Natalia  
6 Barrientos<sup>3</sup>, Matt O'Regan<sup>3</sup>, Carina Johansson<sup>3</sup>, Andrey Koshurnikov<sup>5,6</sup>, Martin  
7 Jakobsson<sup>3</sup>

8 <sup>1</sup> U.S. Geological Survey, Reston, Virginia

9 <sup>2</sup> Rensselaer Polytechnic Institute, Department of Earth & Environmental Sciences,  
10 Troy, New York

11 <sup>3</sup> Department of Geological Sciences and Bolin Centre for Climate Research,  
12 Stockholm University, Stockholm, 10691, Sweden

13 <sup>4</sup> Department of Geoscience, Aarhus University, Aarhus, 8000, Denmark

14 <sup>5</sup> Tomsk National Research Polytechnic University, Tomsk, Russia

15 <sup>6</sup> Moscow State University, Geophysics, Russian Federation

16  
17 *Correspondence to:* Laura Gemery ([lgemery@usgs.gov](mailto:lgemery@usgs.gov))

18 *Keywords:* Arctic Ocean, Quaternary, Sea-ice history, Sediment cores,  
19 Paleobiological proxies, Benthic ostracode assemblages

20  
21  
22 **Abstract**

23  
24 Late Quaternary paleoceanographic changes in the central Arctic Ocean were  
25 reconstructed from a multicore and gravity core from the Lomonosov Ridge (Arctic  
26 Ocean) collected during the 2014 SWERUS-C3 Expedition. Ostracode  
27 assemblages dated by accelerator mass spectrometry (AMS) indicate changing  
28 sea-ice conditions and warm Atlantic Water (AW) inflow to the Arctic Ocean from  
29 ~50 ka to present. Key taxa used as environmental indicators include  
30 *Acetabulastoma arcticum* (perennial sea ice), *Polycope* spp. (productivity and sea  
31 ice), *Krithe hunti* (partially sea-ice free conditions, deep water inflow), and  
32 *Rabilimis mirabilis* (high nutrient, AW inflow). Results indicate seasonally sea-ice  
33 free conditions during Marine Isotope Stage (MIS) 3 (~57-29 ka), rapid deglacial  
34 changes in water mass conditions (15-11 ka), seasonally sea-ice free conditions  
35 during the early Holocene (~10-7 ka) and perennial sea ice during the late  
36 Holocene. Comparisons with faunal records from other cores from the Mendeleev  
37 and Lomonosov Ridges suggest generally similar patterns, although sea-ice cover  
38 during the last glacial maximum may have been less extensive at the southern  
39 Lomonosov Ridge at our core site (~85.15°N, 152°E) than farther north and  
40 towards Greenland. The new data also provide evidence for abrupt, large-scale  
41 shifts in ostracode species depth and geographical distributions during rapid  
42 climatic transitions.

43 **1. Introduction**

44 The observed, rapidly changing environmental conditions in the Arctic Ocean,  
45 including diminishing sea-ice extent and thickness (Stroeve et al., 2012, 2014;  
46 Laxon et al., 2013), glacial retreat (Zemp et al., 2015) and changes in ocean  
47 circulation (Moore et al, 2015), chemistry (Chierici and Fransson 2009; Rabe et al.,



48 2011) and ecology (Grebmeier et al., 2006, 2012; Wassmann et al., 2011), are  
49 only possible to fully assess with a longer time perspective at hand. Such  
50 environmental perspective reaching further back in time is best acquired through  
51 paleoceanographic studies of sediment cores from the Arctic Ocean. This study  
52 examines temporal changes in ostracode indicator species of biological  
53 productivity and sea-ice extent during the last ~50 ka, including Marine Isotope  
54 Stages (MIS) 3, the Last Glacial Maximum (LGM), the deglacial interval and the  
55 Holocene, at about 85.15°N, 152°E on the Lomonosov Ridge in the central Arctic  
56 Ocean. Marine Ostracoda are bivalved Crustacea that inhabit Arctic marine  
57 habitats and whose assemblages (Cronin et al., 1994, 1995, 2010; Poirier et al.,  
58 2012) and shell chemistry (Cronin et al., 2012) have been used extensively as  
59 proxies to reconstruct Arctic paleoceanography.

60  
61 New ostracode faunal analyses are derived from two sediment cores collected on  
62 the Lomonosov Ridge during the 2014 SWERUS-C3 (Swedish – Russian – US  
63 Arctic Ocean Investigation of Climate-Cryosphere-Carbon Interactions) Leg 2  
64 expedition, and results are compared to published faunal records from past  
65 expeditions to the Lomonosov, Mendeleev and Northwind Ridges (Fig. 1a, Table  
66 1). The new sites are located beneath the Transpolar Drift, a surface circulation  
67 pattern that transports sea ice across the central Arctic Ocean from the Siberian  
68 and Laptev seas towards the Fram Strait, and hence influences ice export into the  
69 Nordic Seas and the North Atlantic.

70  
71 The central Arctic Ocean has exhibited significant oceanographic changes over  
72 orbital timescales as reflected in various lithological, geochemical and  
73 micropaleontological proxies (Nørgaard-Pederson et al., 1998; O'Regan et al.,  
74 2008; Marzen et al., 2016). In addition to records of orbitally forced climate  
75 changes, some Arctic Ocean records contain evidence for suborbital changes,  
76 including the prevalence of frequent, rapid geographic range shifts of ecologically  
77 sensitive species. For example, prior studies have documented range shifts in  
78 Arctic benthic foraminifera during the last deglaciation ~15-10 ka (Taldenkova et al.,  
79 2012) and during MIS 3 ~57-29 ka (Polyak et al., 1986; Ishman et al., 1996). In the  
80 new records presented here, evidence for similar range shifts in the ostracode  
81 species *Rabulimys mirabilis* is described, and we briefly discuss these exceptional,  
82 but only partially understood, biological events.

## 83 2. Arctic oceanography

84 The following summary of Arctic water masses and circulation is taken from  
85 Aagaard and Carmack (1989), Anderson et al. (1994), Jones (2001), Olsson and  
86 Anderson (1997), and Rudels et al. (2012 and 2013). Arctic Ocean water masses  
87 include a fresh, cold polar surface layer ([PSW], T= ~0°C to -2°C, S= ~32 to 34),  
88 that is found between ~0 to 50 m, and overlays a warmer, denser water mass of  
89 North Atlantic origin (the Atlantic water [AW], ~200 to 1000 m, T= >0°C, S= ~34.6  
90 to 34.8). One branch of the AW flows into the Arctic Ocean from the Nordic seas  
91 along the eastern Fram Strait off the west coast of Spitsbergen and another branch  
92 flows through the Barents Sea. Bathymetry is a dominant factor in creating  
93 circulation patterns for AW and all deeper water, and a sharp front over the  
94 Lomonosov Ridge near the SWERUS-C3 cores studied here nearly isolates these



95 waters in the Eurasian Basin from the Canadian Basin (Fig. 1b). Into the western  
96 Arctic Ocean, nutrient-rich, low salinity water enters from the North Pacific/Bering  
97 Sea region through the Bering Strait (~53 m). A halocline separates the cold,  
98 fresher water beneath the sea-ice cover from the underlying warmer and saltier  
99 AW.

100 An intermediate-depth water mass below the AW in the Eurasian Basin at ~1000-  
101 1500 m is called the Arctic Intermediate water ([AIW], T= -0.5 to 0°C, S= ~34.6 to  
102 34.8). Below 2000 m, the deep Arctic basins are filled with Arctic Ocean Deep  
103 Water ([AODW], T= -1.0°C to -0.6°C, S= 34.9, Somavilla et al., 2013). Figure 1b  
104 shows a cross section of these major water masses in the eastern and central  
105 basin of the Arctic Ocean near the study site on the Lomonosov Ridge.

### 106 3. Materials and methods

107

#### 108 3.1 Core material and sample processing

109 Cores for this study were obtained during the September 2014 SWERUS-C3 (Leg  
110 2) expedition to the eastern Arctic Ocean aboard Swedish Icebreaker *Oden*. Figure  
111 1 shows the location of multicore SWERUS-L2-32-MC4 (85.14°N, 151.57°E, 837  
112 m) and nearby gravity core SWERUS-L2-32-GC2 (85.15°N, 151.66°E, 828 m) on  
113 the Lomonosov Ridge. These cores are hereafter referred to as 32-MC and 32-  
114 GC, respectively. Both cores were stored at 4°C and sampled at the Department of  
115 Geological Sciences, Stockholm University. Processing of the samples involved  
116 washing the sediment with water through a 63-µm mesh sieve. Core 32-MC was  
117 processed in Stockholm while 32-GC was processed at the U.S. Geological  
118 Survey (USGS) laboratory in Reston, Virginia. Sediment samples (1-cm thick, ~30  
119 g prior to processing) were taken every centimeter in 32-MC along its 32 cm  
120 length. Section 1 (117 cm) of 32-GC was sampled every 2-3 cm (2-cm thick, ~45-  
121 60 g wet weight).

122

123 After processing and oven drying the samples, the residual >125 µm size fraction  
124 was sprinkled on a picking tray and ostracodes were removed to a slide. One  
125 exception for expediency is that specimens of the genus *Polycope* were counted  
126 and not removed from the sediment. A total of ~300 specimens were studied from  
127 each sample of 32-MC. More detailed counts of some samples in 32-MC were  
128 done periodically, where all specimens were picked and/or counted to ensure that  
129 300 specimens provided a representative assemblage. In 32-GC, all specimens  
130 were picked and/or counted in each sample. Ostracodes were present throughout  
131 the entire studied intervals of both 32-MC and down to 62 cm in 32-GC. Planktic  
132 and benthic foraminifers were also present in abundance but not studied.

133

#### 134 3.2 Chronology, reservoir corrections and sedimentation

135 We obtained nine radiocarbon (<sup>14</sup>C) ages from core 32-MC using accelerator mass  
136 spectrometry (AMS) (Fig. 2, Table 2). Most dates were obtained on mollusks  
137 (*Nuculidae* and *Arcidae* spp.), except a few where mollusks and benthic  
138 foraminifera were combined. We obtained two ages from 32-GC using a  
139 combination of mollusks, foraminifera and ostracode shells. The final age models  
140 representing the two cores combined are based on all the calibrated <sup>14</sup>C ages  
141 listed in Table 2. Calibration into calendar years was done using Oxcal4.2 (Bronk



142 Ramsey, 2009) and the Marine13 calibration curve (Reimer et al., 2013). In  
143 addition to the global marine correction of 402 years (Stuiver and Reimer 2010), a  
144  $\Delta R$  value of  $300 \pm 100$   $^{14}\text{C}$  years was used to account for regional reservoir effects  
145 (Reimer and Reimer, 2001).

146  
147 Similar patterns in ostracode assemblages were used to depth align 32-MC and  
148 32-GC and a 3-cm offset was applied to 32-GC. After adding the 3-cm offset to  
149 sample depths of 32-GC, we applied the 32-MC core chronology down to 31.5 cm  
150 core depth (dated at 39.6 ka). The average sedimentation rate was  $\sim 1.5$  cm/ka  
151 which is typical of central Arctic Ocean ridges (Backman et al., 2004; Polyak et al.,  
152 2009).

153  
154 The lower section of 32-GC, from 31.5 cm to 61 cm, is beyond the limit of  
155 radiocarbon dating. However, the litho-stratigraphy of the gravity core can be  
156 readily correlated to other records from the central Lomonosov ridge, where  
157 multiple dating techniques constrain the approximate positions of MIS 4 and 5  
158 boundaries (Jakobsson et al., 2001; O'Regan, 2011). A correlation between  
159 SWERUS-C3 32-GC and AO96/12-1PC was previously presented in Jakobsson et  
160 al. (2016). The correlation is supported by the occurrences in 32-GC of the  
161 calcareous nanofossil *E. huxleyii* (Fig. 2). Based on this longer-term  
162 correlation, sediments between 31 and 61 cm are less than 50 ka. This is  
163 consistent with previous work on the Lomonosov Ridge, revealing a prominent  
164 transition from coarse-grained, microfossil-poor sediments (diamict) into  
165 bioturbated, finer-grained microfossiliferous sediments occurring during MIS 3 at  
166 approximately 50 ka (Spielhagen et al., 2004; Nørgaard-Pederson et al., 2007).

## 167 168 4. Results

### 169 4.1 Ostracode taxonomy and ecology

170 The SWERUS 32 cores contained a total of 13,767 ostracode specimens in 32-MC  
171 and a total of 5,330 specimens in the uppermost 5-62 cm of 32-GC (the top few  
172 centimeters below the seafloor were not recovered in the gravity core). The bottom  
173 54 cm of 32-GC (section 1 from 63-117 cm) was barren of calcareous material.  
174 Twenty-eight ostracode species were identified in 32-MC and 21 species were  
175 identified in 32-GC. Supplementary Tables S1 and S2 provide all species and  
176 genus census data for 32-MC and 32-GC, respectively. Data will also be  
177 accessible at NOAA's [National Centers for Environmental Information \(NCEI,](https://www.ncdc.noaa.gov/paleo-search/)  
178 [https://www.ncdc.noaa.gov/paleo-search/\)](https://www.ncdc.noaa.gov/paleo-search/). The primary sources of taxonomy and  
179 ecology were papers by Cronin et al. (1994, 1995, 2010), Gemery et al. (2015),  
180 Joy and Clark (1977), Stepanova (2006), Stepanova et al. (2003, 2007, 2010),  
181 Whatley et al. (1996, 1998), and Yasuhara et al. (2014).

182  
183 Most ostracodes were identified at the species level except the genera  
184 *Cytheropteron* and *Polycope*. Table 3 provides a list of species included in the  
185 genus-level groups, which was sufficient to reconstruct paleoenvironmental  
186 changes. There are several species of *Cytheropteron* in the deep Arctic Ocean but  
187 they are not ideal indicator species given their widespread modern distributions.  
188 There are at least 8 species of *Polycope* in the Arctic Ocean, but juvenile molts of  
189 *Polycope* species are difficult to distinguish from one another. Most specimens in  
190 32-MC and 32-GC belonged to *P. inornata* Joy & Clark, 1977 and *P. bireticulata*



191 Joy & Clark, 1977. Nonetheless, most *Polycope* species co-occur with one  
192 another, are opportunistic in their ecological strategy, and dominate assemblages  
193 associated with high surface productivity and organic matter flux to the bottom  
194 (Karanovic and Brandão, 2012, 2016).

195  
196 The relative frequency (percent abundance) of individual dominant taxa is plotted  
197 in Figure 3 and listed in Supplementary Table S3. Abundances were computed by  
198 dividing the number of individual species found in each sample by the total number  
199 of specimens found. For 32-MC, using the algorithm for a binomial probability  
200 distribution provided by Raup (1991), ranges of uncertainty (“error bars”) were  
201 calculated at the 95% fractile for the relative frequency in each sample to the  
202 relative frequency of each species and the total specimen count of each sample at  
203 a given core depth (Supplementary Table S4). For this study of the SWERUS-C3  
204 32 cores, our focus was on the following taxa: *Acetabulastoma arcticum*, *Krithe*  
205 *hunti*, *Polycope* spp., *Cytheropteron* spp., *Pseudocythere caudata*, and *Rabilimis*  
206 *mirabilis*. Table 4 provides an overview of pertinent aspects of these species’  
207 ecology that have paleoceanographic application.

208

#### 209 4.2 Temporal patterns in ostracode indicator species from SWERUS-C3 32- 210 MC/GC

211 The faunal patterns in cores from the SWERUS-C3 32-MC/GC sites confirm faunal  
212 patterns occurring over much of the central Arctic Ocean during the last 50 ka,  
213 including MIS 3-2 (~50 to 15 ka), the last deglacial interval (~15 to 11 ka), and the  
214 Holocene (~11 ka to present). We briefly discuss the paleoceanographic  
215 significance of each period in the following sections 4.3 - 4.5 based on the  
216 comparison cores presented in Figs 4 and 5. Relative frequencies of indicator taxa  
217 in cores 32-MC and 32-GC (Fig. 3) show four distinct assemblages, which we refer  
218 to as informal faunal zones following prior workers (Cronin et al., 1995; Poirier et  
219 al., 2012). These are: (1) *Krithe* zone (primary abundance up to 80% during ~45-  
220 42 ka and a secondary abundance of 5-10% during ~42-35 ka); (2) *Polycope* zone  
221 (with abundance of 50 to 75% during ~40-12 ka, also containing a double peak in  
222 abundance of *P. caudata*); (3) *Cytheropteron-Krithe* zone (12-7 ka); and (4)  
223 *Acetabulastoma arcticum* zone (~7 ka-present). Similar patterns are seen in both  
224 the multicore and gravity core. In addition, the ostracode data reveal two *Rabilimis*  
225 *mirabilis* “events,” or intervals containing high proportions of this shallow water  
226 species (dated at ~45-36 ka and 9-8 ka).

227

228 Figures 4 and 5 compare the new SWERUS-C3 results from 32-MC with published  
229 data from box and multicores from the Lomonosov and Mendeleev Ridges,  
230 respectively, covering a range of water depths from 700-1990 m. Most records  
231 extend back to at least 45 ka, and the age model for each core site is based on  
232 calibrated radiocarbon ages from that site (Cronin et al., 2013, 2010; Poirier et al.,  
233 2012).

234

#### 235 4.3 MIS 3-2 (~50-15 ka)

236 A strong peak in the abundance of *Krithe hunti* (Fig. 3) is seen in 32-GC sediments  
237 estimated to be ~45-42 ka in age. A similar peak of lower but still significant  
238 abundance also occurs in sediments dated between 42 and 35 ka, and this is  
239 consistent with other cores on the Mendeleev Ridge and particularly on the



240 Lomonosov Ridge (Figs 4, 5). Prior studies of Arctic ostracodes have shown that  
241 *Krithe* typically signifies cold well-ventilated deep water and perhaps low food  
242 supply (Poirier et al., 2012 and references therein). *Krithe* is also a dominant  
243 component (>30%) of North Atlantic Deep Water (NADW) in the subpolar North  
244 Atlantic Ocean. Its abundance varies during glacial-interglacial cycles, reaching  
245 maxima during interglacial and interstadial periods (Alvarez Zarikian et al., 2009).  
246 Peaks in the abundance of *Krithe* in the Arctic Ocean probably signify faunal  
247 exchange between the North Atlantic Ocean and the Greenland-Norwegian Seas  
248 through the Denmark Strait and Iceland Faroes Ridge and the Greenland-  
249 Norwegian Seas and the central Arctic through the Fram Strait. In other Arctic  
250 Ocean cores, the ostracode genus *Henryhowella* is often associated with *Krithe*  
251 sp. in sediments dated between ~50 to 29 ka (MIS 3), and its absence in the 32-  
252 MC/GC cores may reflect the relatively shallow depth at the coring site.

253

254 *A. arcticum* is present in low abundance (~5%) in sediment dated at ~42 to 32 ka  
255 in 32-MC/GC (Fig. 3), signifying intermittent perennial sea ice. A *Krithe* to *Polycope*  
256 shift occurs at ~35-30 ka. This “K-P shift” is a well documented Arctic-wide  
257 transition (Cronin et al., 2014) that has paleoceanographic significance as well as  
258 biostratigraphic utility. *Polycope* is clearly the dominant genus group from sediment  
259 dated ~40-12 ka in 32-MC/GC and all sites on the Lomonosov and Mendeleev  
260 Ridges (Figs. 4, 5), signifying high productivity likely due to an intermittent, rapidly  
261 oscillating sea-ice edge at the surface. *P. caudata* has varying percentages (3-  
262 14%) in sediment dated ~40-12 ka, depending on the site. *Cytheropteron* spp. is  
263 present in moderate abundance (20-30%) in sediment dated ~35-15 ka.

264

#### 265 4.4 The Last Deglacial Interval (~15 to 11 ka)

266 The major shift from *Polycope*-dominated to *Cytheropteron-Krithe*-dominated  
267 assemblages occurs in sediment dated ~15-12 ka in 32-MC/GC and other  
268 Lomonosov and Mendeleev Ridge cores. Both *Cytheropteron* and *Krithe* are  
269 typical faunas in NADW. Although low sedimentation rates prevent precise dating  
270 of this shift, it almost certainly began ~14.5 ka at the Bølling-Allerød warming  
271 transition. Because the Bering Strait had not opened yet (Jakobsson et al., 2017),  
272 this faunal shift must have been related to one or several of the following changes:  
273 (1) atmospheric warming; (2) strong Atlantic Water inflow through the Barents Sea;  
274 and (3) strong Atlantic Water inflow through the eastern Fram Strait. *A. arcticum*  
275 is absent or rare (<2% of the assemblage) in sediment dated ~15-12 ka, suggesting  
276 minimal perennial sea ice cover and probably summer sea-ice free conditions  
277 during late deglacial warming.

278

#### 279 4.5 The Holocene (~11 to Present)

280 *Krithe* and *Cytheropteron* remain abundant in sediment dated ~10-7 ka (early  
281 Holocene) across most of the central Arctic Basin, signifying continued influence of  
282 water derived from the North Atlantic Ocean (Figs. 4, 5). *A. arcticum* (which  
283 represents the *A. arcticum* zone) increases to >6-8% abundance beginning in  
284 sediment dated ~7 ka, and increases to >10% abundance in sediment dated ~3  
285 ka. This increase in abundance is correlated with an increase in perennial-sea ice,  
286 and is more prominent in Lomonosov Ridge cores than in cores from the  
287 Mendeleev Ridge (most likely due to more persistent perennial sea ice cover over  
288 the Lomonosov Ridge sites). The inferred middle to late Holocene development of



289 perennial sea ice is consistent with interpretations from other sea-ice proxies (Xiao  
290 et al., 2015) and with the transition from an early-middle Holocene “thermal  
291 maximum” (Kaufman et al., 2004, 2016) to cooler conditions during the last few  
292 thousand years.

293

## 294 5. Discussion

295

### 296 5.1 Faunal events in the Arctic Ocean

297 Major paleoceanographic shifts inferred from ostracode assemblages presented  
298 above signify orbital and, at least at low resolution, millennial events during the last  
299 50 ka. In general, the data confirm the sensitivity of Arctic benthic fauna to  
300 relatively large climate transitions, such as those seen in benthic foraminifera  
301 during the last deglacial and Holocene intervals from the Laptev Sea (Taldenkova  
302 et al., 2008, 2013) and the Beaufort Sea and Amundsen Gulf (Scott et al., 2009).  
303 These records provide a useful context for understanding orbital-scale Arctic  
304 faunal variability during the last 500 ka, as seen in benthic foraminifera and  
305 ostracodes (Cronin et al., 2014; Marzen et al., 2016).

306

307 These millennial faunal changes seem to be distinct from microfaunal events in  
308 which a species is found in certain stratigraphic intervals in sediment cores located  
309 far outside that species normal depth and/or geographic range. One example is  
310 *Bulimina aculeata* (Polyak et al., 1986, 2004; Ishman et al., 1996), a species that  
311 occurs in narrow (few cm thick) stratigraphic intervals such that it serves as a  
312 useful biostratigraphic marker in sediment dated ~96-71 ka (MIS 5c-5a; Cronin et  
313 al., 2014). As reviewed by (Polyak et al., 2004), *B. aculeata* is almost completely  
314 absent from the modern Arctic Ocean, and its widespread occurrence as a double  
315 peak in abundance across much of the Arctic Ocean in sediment dated ~96-71 ka  
316 (late MIS 5) must signify a unique but still poorly understood oceanographic  
317 situation. Polyak et al. (2004) noted a similar stratigraphic situation for  
318 *Epistominella exigua* and other benthic foraminiferal species in the western Arctic  
319 Ocean. In the eastern Arctic Ocean, Wollenburg et al. (2001) also discusses how  
320 peaks in abundance of *Melonis zaandami* represent brief paleoceanographic  
321 events. These and other examples where species have pulse-like spikes in  
322 abundance and geographically widespread stratigraphic distributions signify brief,  
323 large-scale changes in species dominance. The causes of such events suggests a  
324 rapid environmental change, such as changing sea ice cover or periods of  
325 enhanced surface-ocean productivity with a food supply flux to the ocean bottom.

326

### 327 5.2 *Rabilimis mirabilis*

328 The distribution of the ostracode *Rabilimis mirabilis* in SWERUS-C3 32-MC/GC  
329 and other Arctic cores represents a similar pattern to that seen for *B. aculeata*, *E.*  
330 *exigua*, and *M. zaandami*, when a brief, uncharacteristic yet significant faunal  
331 dominance of a taxa is indicative of rapid environmental change. In SWERUS-C3  
332 32-MC/GC, *R. mirabilis* occurs in sediment dated ~45-36 ka (MIS 3) with  
333 abundance reaching 60%, and again in sediment dated ~9-8 ka (early Holocene)  
334 with abundance reaching 41-55%. These two intervals of high abundance signify  
335 an unusual stratigraphic appearance of a shallow-water species in a relatively  
336 deep-water (837 m) core site.

337



338 The modern circum-Arctic distribution of *R. mirabilis* is confined to relatively  
339 shallow (<200 m) water depths (Fig. 6a, b, and c; Hazel, 1970; Neale and Howe,  
340 1975; Taldenkova et al., 2005; Stepanova, 2006; Gemery et al., 2015). *R. mirabilis*  
341 can also tolerate a range of salinities, explaining its presence in regions near river  
342 mouths with reduced salinity (Fig. 6a).

343  
344 *Rabilimis mirabilis* also occurs in 2014 SWERUS-C3 multicore top samples at  
345 deeper than usual depths on the Eastern Siberian Sea slope. Examples of these  
346 occurrences are listed in Supplementary Table S5 and include SWERUS-C3  
347 Cores 23-MC4 (4%, 522 m); 18-MC4 (18%, 349 m); 16-MC4 (11%, 1023 m); 15-  
348 MC4 (41%, 501 m) and 14-MC4 (70%, 837 m). These locations correspond to the  
349 summer sea-ice edge that has receded during recent decades over the  
350 Lomonosov Ridge and may be indicative of warming and/or surface-to-bottom  
351 nutrient flux.

352  
353 Data from the current study, from Cronin et al. (2014) and other Arctic core studies  
354 reveal new information about the stratigraphic occurrence of *R. mirabilis* (Fig. 7a,  
355 7b, Table 5). In the central Arctic Ocean, *R. mirabilis* occurs on the Lomonosov  
356 Ridge (96-12-1PC), the Mendeleev Ridge (P1-94-AR-PC10) and Northwind Ridge  
357 (P1-92-AR-PC40) and in longer cores on the Lomonosov and Northwind Ridge  
358 (Fig 7b). Age models for these sites suggest a range extension of *R. mirabilis* into  
359 deeper water (700 to 1673 m) during interstadial periods (MIS 5c, 5a, 3). *R.*  
360 *mirabilis*' abundance reaches 40-50% of the total assemblage at Lomonosov  
361 Ridge site 96-12-1PC at a water depth of 1003 m. Such anomalously high  
362 percentages of well-preserved adult and juvenile specimens of *R. mirabilis* indicate  
363 that they were not brought to the site through sediment transport from the shelf.  
364 Instead, we interpret the *R. mirabilis* events to represent in-situ populations.

365  
366 Although not all *R. mirabilis* events are synchronous, most occur in sediment dated  
367 ~96-71 ka (late MIS 5) and at SWERUS-C3 coring sites of 32-MC and 32-GC in  
368 sediment dated 45-36 ka and ~9-8 ka (early Holocene). These *R. mirabilis* events  
369 are correlated with interglacial/interstadial periods that experienced summer sea-  
370 ice free and/or sea-ice edge environments where there may have been enhanced  
371 flux of surface-to-bottom organic matter. We hypothesize that the locations of the  
372 *R. mirabilis* events on the southern Lomonosov and Mendeleev Ridges received  
373 an influx of nutrient-enriched water through the Bering Strait into the western Arctic  
374 Ocean. However, to confirm the paleoceanographic significance of *R. mirabilis*  
375 migration events, additional study of cores from Arctic margins is required.

376

## 377 6. Conclusions

378

379 SWERUS-C3 Cores 32-MC and 32-GC on the Lomonosov Ridge are  
380 characterized by fluctuating dominance of key ostracode taxa that indicate various  
381 water mass regimes from ~50 ka to present (MIS 3-1). Key indicator taxa and their  
382 associations with specific water masses show the following four major ostracode  
383 assemblage changes in Cores 32-MC/GC as characterized by peaks in dominant  
384 ostracode taxa: (1) *Krithe* zone (~45-35 ka); (2) *Polycope* zone (~40-12 ka); (3)  
385 *Cytheropteron-Krithe* zone (~12-7 ka); and (4) *Acetabulastoma arcticum* zone (~7  
386 ka-present). These benthic faunal events, and unusual events like *Rabilimis*



387 *mirabilis* shelf-to-ridge migration events, indicate abrupt changes in Eurasian Basin  
388 environmental conditions related to sea ice extent and the relative strength of  
389 Atlantic Water influx to the Arctic Ocean.

#### 390 Acknowledgements

391 We are grateful to the crew of Icebreaker *Oden* and the SWERUS-C3 Scientific  
392 Team. Thanks to A. Ruefer for assistance with sample processing. This  
393 manuscript benefitted from reviews by C. Swezey and M. Toomey. This study was  
394 funded by the U.S. Geological Survey Climate R&D Program. Any use of trade,  
395 firm, or product names is for descriptive purposes only and does not imply  
396 endorsement by the U.S. Government. Data presented in the article acquired  
397 during the 2014 SWERUS-C3 expedition are available through the Bolin Centre for  
398 Climate Research database: <http://bolin.su.se/data/>.

399  
400 Fig 1. a.) International Bathymetric Chart of the Arctic Ocean showing the location  
401 of this study's primary sediment cores on the Lomonosov Ridge (red star: 32-GC2  
402 and 32-MC4), and other core sites discussed in this paper (black circles, white  
403 circles). (See Table 1 for supplemental core data.) White circles designate cores  
404 that contain *Rabilimis mirabilis* events. Red arrows show generalized circulation  
405 patterns of warm Atlantic water in the Arctic Ocean. Transect line through the map  
406 from "1" in the Chukchi Sea to "2" in the Barents Sea shows direction of  
407 temperature profile in Fig1b.

408 b.) Cross section of modern Arctic Ocean temperature profile from showing major  
409 water masses. PSW: polar surface water, AL: Atlantic layer, AIW: Arctic  
410 intermediate Water, AODW: Arctic Ocean Deep water. Ocean Data View Source:  
411 Schlitzer, 2012. Ocean Data View: <http://odv.awi.de>

412  
413 Fig. 2 Chronology and stratigraphy of SWERUS-32-GC and 32-MC. Bulk density  
414 and magnetic susceptibility profiles for 32GC were previously correlated to the  
415 well-dated 96-12-1PC core by Jakobsson et al. (2016). Bulk density primarily  
416 reflects changes in grain size, with coarser material having a higher density than  
417 finer grained material. The overall position of MIS 5 is supported by the occurrence  
418 of *E. huxleyi*. The chronology for the upper 30-35 cm is based on radiocarbon  
419 dating in both 32-MC and 32-GC. Beyond the range of radiocarbon dating, an  
420 extrapolation to the inferred position of MIS 3/4 boundary (57 ka at 105 cm) is  
421 applied.



422

423 Fig 3. Relative frequencies (percent abundance) of dominant taxa in SWERUS-C3  
424 32-MC and 32-GC. The y-axis shows the modeled, mean age during a 2-sigma  
425 range of uncertainty.

426

427 Fig 4. Relative frequencies (percent abundance) of dominant taxa in SWERUS  
428 32-MC (dotted line) compared to other Lomonosov Ridge cores 2185, 2179 and  
429 AOS94 28 (Poirier et al., 2012).

430

431 Fig 5. Relative frequencies (percent abundance) of dominant taxa in SWERUS  
432 32-MC (dotted line) compared to other Mendeleev Ridge cores AOS94 8 (Poirier et  
433 al., 2012), AOS94 12, and HLY6.

434

435 Fig 6. a.) Occurrence map of *Rabilimis mirabilis* in the Arctic Ocean and  
436 surrounding seas based on 1340 modern surface samples in the Arctic Ostracode  
437 Database (AOD; Gemery et al., 2015).

438 b.) Modern depth and c.) latitudinal distribution of *R. mirabilis* based on 1340-  
439 modern surface samples in the AOD (Gemery et al., 2015).

440

441 Fig 7. a.) Relative frequency (percent abundance) of *R. mirabilis* in SWERUS-32  
442 cores and in central Arctic Ocean cores, 160 ka to present. b.) *R. mirabilis* in core  
443 LOMROG07-04 from 260 ka to present and in core P1-92-AR-PC30 from 340 ka to  
444 present.

445

#### 446 References

447

448 Aagaard, K. and Cannack, E.C.: The role of sea ice and other fresh water in the  
449 Arctic circulation, J Geophys Res, 94(14), 485-498,  
450 doi:10.1029/JC094iC10p14485, 1989.

451

452 Anderson, L.G., Olsson, K., Skoog, A.: Distribution of dissolved inorganic and  
453 organic carbon in the Eurasian Basin of the Arctic Ocean. In: O. M. Johannessen,  
454 R. D. Muench, and J. E. Overland, (eds.), The Polar Oceans and their Role in  
455 Shaping the Global Environment, Geophysical Monograph 85, American  
456 Geophysical Union, 525-562, 1994.

457

458 Anderson, L.G., Björk, G., Jutterström, S., Pipko, I., Shakhova, N., Semiletov, I.  
459 and Wählström, I.: East Siberian Sea, an Arctic region of very high biogeochemical



- 460 activity, *Biogeosciences*, 8(6), 1745–1754, doi:10.5194/bg-8-1745, 2011.
- 461 Backman, J., Jakobsson, M., Lovlie, R., Polyak, L., and Febo, L. A.: Is the central  
462 Arctic Ocean a sediment starved basin?, *Quaternary Sci Rev*, 23, 1435-1454,  
463 2004.
- 464 Brady, G. S.: A Monograph of the Recent British Ostracoda, *Transact Linn Soc*  
465 London, 26(2), 353–495, 1868.
- 466 Brady, G.S., Crosskey, H.W., Robertson, D.: A Monograph of the Post-Tertiary  
467 Entomostraca of Scotland, Including Species from England and Ireland,  
468 *Paleontograph Soc London*, 28, 1–232, 1874.
- 469 Bronk Ramsey, C.: Bayesian Analysis of Radiocarbon Dates, *Radiocarbon*, 51(1),  
470 337–360, doi:10.2458/azu\_js\_rc.v51i1.3494, 2009.
- 471 Chierici, M. and Fransson, A.: Calcium carbonate saturation in the surface water of  
472 the Arctic Ocean: undersaturation in freshwater influenced shelves,  
473 *Biogeosciences*, 6, 2421-2431, doi:10.5194/bg-6-2421-2009, 2009.
- 474 Cronin, T. M., DeNinno, L. H., Polyak, L., Caverly, E. K., Poore, R. Z., Brenner, A.,  
475 Rodriguez-Lazaro, J. and Marzen, R. E.: Quaternary ostracode and foraminiferal  
476 biostratigraphy and paleoceanography in the western Arctic Ocean, *Mar*  
477 *Micropaleontol*, 111, 118-133, 2014.
- 478 Cronin, T.M., Polyak L., Reed, D., Kandiano, E.S., Marzen, R.E., Council, E.A.: A  
479 600-ka Arctic sea-ice record from Mendeleev Ridge based on ostracodes,  
480 *Quaternary Sci Rev*, 79, 157-167, 2013.
- 481 Cronin, T.M., Dwyer, G.S., Farmer, J., Bauch, H.A., Spielhagen, R.F., Jakobsson,  
482 M., Nilsson, J., Briggs, W.M., Stepanova, A.: Deep Arctic Ocean warming during  
483 the Last Glacial cycle, *Nat Geosci*, 5, 631-634, 2012.
- 484 Cronin, T.M., Gemery, L., Briggs, W.M. Jr., Jakobsson, M., Polyak, L., Brouwers,  
485 E.M.: Quaternary Sea-ice history in the Arctic Ocean based on a new Ostracode  
486 sea-ice proxy, *Quaternary Sci Rev*, 1-15, doi:10.1016/j.quascirev.2010.05.024,  
487 2010.
- 488 Cronin, T. M., DeMartino, D. M., Dwyer, G. S. and Rodriguez-Lazaro, J.: Deep-sea  
489 ostracode species diversity: response to late Quaternary climate change, *Mar*  
490 *Micropaleontol*, 37, 231-249, 1999.
- 491 Cronin, T.M., Holtz, T.R., Jr., Stein, R., Spielhagen, R., Fütterer, D. and  
492 Wollenberg, J.: Late Quaternary paleoceanography of the Eurasian Basin, Arctic  
493 Ocean, *Paleoceanography*, 10(2), 259–281, doi:10.1029/94PA03149, 1995.
- 494 Cronin, T.M., Holtz, T.R., Jr. and Whatley, R.C.: Quaternary Paleoceanography of  
495 the deep Arctic Ocean based on quantitative analysis of Ostracoda, *Mar Geol*,  
496 19(3–4), 305–332, doi:10.1016/0025-3227(94)90188-0, 1994.



- 497 Feyling-Hanssen, R.W.: Foraminiferal stratigraphy in the Plio- Pleistocene Kap  
498 København Formation, North Greenland, Meddelelser om Grønland, Geoscience,  
499 24, 1-32, 1990.
- 500 Gemery, L., Cronin, T. M., Briggs Jr, W. M., Brouwers, E. M., Schornikov, E. I.,  
501 Stepanova, A., Wood, A. M., and Yasuhara, M.: An Arctic and Subarctic ostracode  
502 database: biogeographic and paleoceanographic applications, Hydrobiologia, 1-37,  
503 2016.
- 504 Grebmeier, J. M.: Shifting Patterns of Life in the Pacific Arctic and Sub-Arctic  
505 Seas, *Annu Rev Mar Sci*, 4, 63-78, 2012.
- 506 Grebmeier, J.M., Overland, J.E., Moore, S.E., Farley, E.V., Carmack, E.C.,  
507 Cooper, L.W., Frey, K.E., Helle, J.H., McLaughlin, F.A. and McNutt, S.L.: A major  
508 ecosystem shift in the northern Bering Sea, *Science*, 311(5766),1461-1464, doi:  
509 [10.1126/science.1121365](https://doi.org/10.1126/science.1121365), 2006.  
510
- 511 Hazel, J.E.: Atlantic continental shelf and slope of the United States-ostracode  
512 zoogeography in the southern Nova Scotian and northern Virginian faunal  
513 provinces, U.S. Geological Survey Professional Paper, 529-E, E1-E21, 1970.
- 514 Ishman, S. E. and Foley, K. M.: Modern benthic foraminifer distribution in the  
515 Amerasian Basin, Arctic Ocean, *Micropaleontology*, 42, 206-220, 1996.
- 516 Jakobsson, M., Pearce, C., Cronin, T.M., Backman, J., O'Regan, M., Anderson,  
517 L.G., Barrientos, N., Björk, G., Coxall, H., Mayer, L.A., Mörth, C.-M., Nilsson, J.,  
518 Rattray, J.E., Stranne, C., Semiletov, I.: Post-glacial flooding of the Beringia Land  
519 Bridge dated to 11,000 cal yrs BP based on new geophysical and sediment record,  
520 *Climate of the Past*, **NEED REF** 2017.
- 521 Jakobsson, M., Nilsson, J., Anderson, L.G., Backman, J., Björk, G., Cronin, T.M.,  
522 Kirchner, N., Koshurnikov, A., Mayer, L., Noormets, R., O'Regan, M., Stranne, C.,  
523 Ananiev, R., Barrientos Macho, N., Cherniykh, D., Coxall, H., Eriksson, B., Floden,  
524 T., Gemery, L., Gustafsson, O., Jerram, K., Johansson, C., Khortov, A.,  
525 Mohammad, R., and Semiletov, I.: Evidence for an ice shelf covering the central  
526 Arctic Ocean during the penultimate glaciation, *Nature Communications*, 7,  
527 doi:10.1038/ncomms10365, 2016.
- 528 Jones, E. P.: Circulation in the Arctic Ocean, *Polar Res*, 20, 139-146, 2001.
- 529 Joy, J. A. and Clark, D.L.: The distribution, ecology and systematics of the benthic  
530 Ostracoda of the central Arctic Ocean, *Micropaleontology*, 23, 129–154. 1977.
- 531 Karanovic, I. and Brandão, S. N.: The genus *Polycope* (Polycopidae, Ostracoda) in  
532 the North Atlantic and Arctic: taxonomy, distribution, and ecology, *Syst Biodivers*,  
533 14, 198-223, 2016.
- 534 Karanovic, I. and Brandão, S. N.: Review and phylogeny of the Recent  
535 Polycopidae (Ostracoda, Cladocopina), with descriptions of nine new species, one



- 536 new genus, and one new subgenus from the deep South Atlantic, *Mar Biodivers*,  
537 42, 329-393, 2012.
- 538 Kaufman, D. S., Axford, Y. L., Henderson, A. C. G., McKay, N. P., Oswald, W. W.,  
539 Saenger, C., Anderson, R. S., Bailey, H. L., Clegg, B., Gajewski, K., Hu, F. S.,  
540 Jones, M. C., Massa, C., Routson, C. C., Werner, A., Wooller, M. J., and Yu, Z. C.:  
541 Holocene climate changes in eastern Beringia (NW North America) - A systematic  
542 review of multi-proxy evidence, *Quaternary Sci Rev*, 147, 312-339, 2016.
- 543 Kaufman, D. S., Ager, T. A., Anderson, N. J., Anderson, P. M., Andrews, J. T.,  
544 Bartlein, P. J., Brubaker, L. B., Coats, L. L., Cwynar, L. C., Duvall, M. L., Dyke, A.  
545 S., Edwards, M. E., Eisner, W. R., Gajewski, K., Geirsdottir, A., Hu, F. S.,  
546 Jennings, A. E., Kaplan, M. R., Kerwin, M. N., Lozhkin, A. V., MacDonald, G. M.,  
547 Miller, G. H., Mock, C. J., Oswald, W. W., Otto-Bliesner, B. L., Porinchu, D. F.,  
548 Ruhland, K., Smol, J. P., Steig, E. J., and Wolfe, B. B.: Holocene thermal  
549 maximum in the western Arctic (0-180 degrees W), *Quaternary Sci Rev*, 23, 529-  
550 560, 2004.
- 551 Laxon, S.W., Giles, K.A., Ridout, A.L., Wingham, D.J., Willatt, R., Cullen, R., Kwok,  
552 R., Schweiger, A., Zhang, J., Haas, C., Hendricks, S., Krishfield, R., Kurtz, N.,  
553 Farrell, S.L. and Davidson, M.: CryoSat estimates of Arctic sea ice volume,  
554 *Geophys Res Lett*, 40, doi:10.1002/grl.50193, 2013.
- 555 Marzen, R. E., DeNinno, L. H. and Cronin, T. M.: Calcareous microfossil-based  
556 orbital cyclostratigraphy in the Arctic Ocean, *Quaternary Sci Rev*, 149, 109-121,  
557 2016.
- 558  
559 Moore, G. W. K., Våge, K., Pickart, R. S. and Renfrew, I. A.: Decreasing intensity  
560 of open-ocean convection in the Greenland and Iceland seas, *Nature Climate*  
561 *Change*, doi: [10.1038/nclimate2688](https://doi.org/10.1038/nclimate2688), 2015.
- 562 National Oceanic and Atmospheric Administration's National Centers for  
563 Environmental Information, [https://www.ncdc.noaa.gov/data-](https://www.ncdc.noaa.gov/data-access/paleoclimatology-data/datasets)  
564 [access/paleoclimatology-data/datasets](https://www.ncdc.noaa.gov/data-access/paleoclimatology-data/datasets)
- 565 Neale, J. W. and Howe, H.V.: The marine Ostracoda of Russian Harbour, Novaya  
566 Zemlya and other high latitude faunas, *Bulletin of American Paleontology*, 65(282),  
567 381-431, 1975.
- 568 Nørgaard-Pedersen, N., Mikkelsen, N., Lassen, S. J., Kristoffersen, Y., Sheldon,  
569 E.: Reduced sea ice concentrations in the Arctic Ocean during the last interglacial  
570 period revealed by sediment cores off northern Greenland, *Paleoceanography*, 22,  
571 PA1218, doi:10.1029/2006PA001283, 2007.
- 572 Nørgaard-Pederson, N., Spielhagen, R.F., Erlenkeuser, H., Grootes, P.M.,  
573 Heinemeier, J., Knies, J.: Arctic Ocean during the Last Glacial Maximum: Atlantic  
574 and polar domains of surface water mass distribution and ice cover,  
575 *Paleoceanography*, 18(3), 1063, doi:10.1029/2002PA000781, 2003.



- 576 Olsson, K. and Anderson, L.G.: Input and biogeochemical transformation of  
577 dissolved carbon in the Siberian shelf seas, *Cont Shelf Res*, 17(7), 819–833, 1997.
- 578 O'Regan, M.: Late Cenozoic paleoceanography of the central Arctic Ocean. *IOP*  
579 *Conf. Series: Earth and Environmental Science* 14, doi:10.1088/1755-  
580 1315/14/1/012002, 2011.
- 581  
582 O'Regan, M., Moran, K., Backman, J., Jakobsson, M., Sangiorgi, F., Brinkhuis, H.,  
583 Pockalny, R., Skelton, A., Stickley, C., Koc, N., Brumsack, H. J., and Willard, D.:  
584 Mid-Cenozoic tectonic and paleoenvironmental setting of the central Arctic Ocean,  
585 *Paleoceanography*, 23, 2008.
- 586  
587 Penney, D.N.: Late Pliocene to Early Pleistocene ostracod stratigraphy and  
588 palaeoclimate of the Lodin Elv and Kap Kobenhavn formations, East Greenland,  
589 *Palaeogeogr, Palaeoclimatol, Palaeoecol*, 101, 49-66, 1993.
- 590 Penney, D.N.: Quaternary ostracod chronology of the central North Sea: The  
591 record from BH 81/29, *Courier Forschungs-Institut Senckenberg*, 123, 97-109,  
592 1990.
- 593 Poirier, R. K., Cronin, T. M., Briggs, W. M. and Lockwood, R.: Central Arctic  
594 paleoceanography for the last 50 kyr based on ostracode faunal assemblages, *Mar*  
595 *Micropaleontol*, 101, 194-194, 2012.
- 596 Polyak, L., Bischof, J., Ortiz, J., Darby, D., Channell, J., Xuan, C., Kaufman, D.,  
597 Lovlie, R., Schneider, D., Adler, R.: Late Quaternary stratigraphy and  
598 sedimentation patterns in the western Arctic Ocean, *Global Planet Change*, 68,5–  
599 17, 2009.
- 600 Polyak, L.V.: New data on microfauna and stratigraphy of bottom sediments of the  
601 Mendeleev Ridge, Arctic Ocean. In: Andreev, S.I. (Ed.), *Sedimentogenes i*  
602 *konkrecoobrazovanie v okeane (Sedimentogenesis and nodule-formation in the*  
603 *Ocean)*. *Sevmorgeologia*, Leningrad, 40-50 (in Russian), 1986.
- 604 Polyak, L., Curry, W. B., Darby, D. A., Bischof, J., and Cronin, T. M.: Contrasting  
605 glacial/interglacial regimes in the western Arctic Ocean as exemplified by a  
606 sedimentary record from the Mendeleev Ridge, *Palaeogeogr, Palaeoclimatol*, 203, 73-  
607 93, 2004.
- 608 Polyak, L., Alley, R.B., Andrews, J.T., Brigham-Grette, J., Darby, D., Dyke, A.,  
609 Fitzpatrick, J.J., Funder, S., Holland, M., Jennings, A., Miller, G.H., Savelle, J.,  
610 Serreze, M., White, J.W.C. and Wolff, E.: History of Sea Ice in the Arctic,  
611 *Quaternary Sci Rev*, 29, 1757-1778, 2010.
- 612 Rabe, B., Karcher, M., Schauer, U., Toole, J.M., Krishfield, R.A., Pisarev, S.,  
613 Kauker, F., Gerdes, R., Kikuchi, T.: An assessment of Arctic Ocean freshwater  
614 content changes from the 1990s to the 2006–2008 period. *Deep Sea Research*  
615 *Part I: Oceanographic Research Papers*, 58(2), 173, doi:  
616 [10.1016/j.dsr.2010.12.002](https://doi.org/10.1016/j.dsr.2010.12.002), 2011.



- 617 Raup, D.M.: The future of analytical paleobiology, In: Gilinsky, N.L., Signor, P.W.  
618 (Eds.), *Analytical Paleobiology: Paleontological Society Short Courses in*  
619 *Paleontology*, 4, 207–216, 1991.
- 620 Reimer, P. J. and Reimer, R. W.: A marine reservoir correction database and on-  
621 line interface, *Radiocarbon*, 43(2A), 461–463, doi:10.2458/azu\_js\_rc.43.3986,  
622 2001.  
623
- 624 Reimer, P. J., Bard, E., Bayliss, A., Beck, J. W., Blackwell, P. G., Bronk Ramsey,  
625 C., Grootes, P. M., Guilderson, T. P., Hafliðason, H., Hajdas, I., Hatté, C., Heaton,  
626 T. J., Hoffmann, D. L., Hogg, A. G., Hughen, K. A., Kaiser, K. F., Kromer, B.,  
627 Manning, S. W., Niu, M., Reimer, R. W., Richards, D. A., Scott, E. M., Southon, J.  
628 R., Staff, R. A., Turney, C.S.M. and Plicht, J. van der: IntCal13 and Marine13  
629 Radiocarbon Age Calibration Curves 0–50,000 Years cal BP, *Radiocarbon*, 55(4),  
630 1869–1887, doi:10.2458/azu\_js\_rc.55.16947, 2013.
- 631 Repenning, C.A., Brouwers, E.M., Carter, L.D., Marincovich Jr., L. and Ager, T.A.:  
632 The Beringian ancestry of *Phenacomys* (Rodentia: Cricetidae) and the beginning  
633 of the modern Arctic Ocean Borderland biota, *U.S. Geological Survey Bulletin*,  
634 1687, 1-31, 1987.
- 635 Rudels, B., Schauer, U., Bjork, G., Korhonen, M., Pisarev, S., Rabe, B. and  
636 Wisotzki, A.: Observations of water masses and circulation with focus on the  
637 Eurasian Basin of the Arctic Ocean from the 1990s to the late 2000s, *Ocean Sci*, 9,  
638 147-169, 2013.
- 639 Rudels, B.: Arctic Ocean circulation and variability - advection and external forcing  
640 encounter constraints and local processes, *Ocean Sci*, 8, 261-286, 2012.
- 641 Schornikov, E. I.: *Acetabulastoma*—a new genus of ostracodes, ectoparasites of  
642 Amphipoda, *Zoologicheskij Zhurnal*, (in Russian), 49, 132–1143, 1970.
- 643 Scott, D. B., Schell, T., St-Onge, G., Rochon, A., and Blasco, S.: Foraminiferal  
644 assemblage changes over the last 15,000 years on the Mackenzie-Beaufort Sea  
645 Slope and Amundsen Gulf, Canada: Implications for past sea ice conditions,  
646 *Paleoceanography*, 24, 2009.
- 647 Siddiqui, Q.A.: The Iperk Sequence (Plio-Pleistocene) and its Ostracod  
648 Assemblages in the Eastern Beaufort Sea. In: T. Hanai, N. Ikeya and K. Ishizaki  
649 (eds.), *Evolutionary Biology on Ostracoda*, Proc. Ninth Int Symp Ostracoda,  
650 Kodansha, Tokyo, pp. 533-540, 1988.
- 651 Somavilla, R., Schauer, U. and Budeus, G.: Increasing amount of Arctic Ocean  
652 deep waters in the Greenland Sea, *Geophys Res Lett*, 40, 4361-4366, 2013.
- 653 Spielhagen, R. F., Baumann, K. H., Erlenkeuser, H., Nowaczyk, N. R., Norgaard-  
654 Pedersen, N., Vogt, C., and Weiel, D.: Arctic Ocean deep-sea record of northern  
655 Eurasian ice sheet history, *Quaternary Sci Rev*, 23, 1455-1483, 2004.  
656



- 657 Stepanova, A., Taldenkova, E., Bauch, H.A.: Late Saalian–Eemian ostracods from  
658 the northern White Sea region, *Joanea Geol Paläont*, 11, 196-198 (abstract only),  
659 2011.
- 660 Stepanova, A. Y., Taldenkova, E. E., Bauch, H. A.: Arctic quaternary ostracods  
661 and their use in paleoreconstructions, *Paleontol J+*, 44, 41-48, 2010.
- 662 Stepanova, A., Taldenkova, E., Simstich, J., Bauch, H.A.: Comparison study of the  
663 modern ostracod associations in the Kara and Laptev seas: Ecological aspects,  
664 *Marine Micropaleontology*, 63, 111-142, 2007.
- 665 Stepanova, A. Y.: Late Pleistocene-Holocene and Recent Ostracoda of the Laptev  
666 Sea and their importance for paleoenvironmental reconstructions, *Paleontol J+*, 40,  
667 S91-S204, 2006.
- 668 Stepanova, A., Taldenkova, E., Bauch, H.A.: Recent Ostracoda of the Laptev Sea  
669 (Arctic Siberia): taxonomic composition and some environmental implications,  
670 *Marine Micropaleontology*, 48(1-2), 23-48, 2003.
- 671 Stroeve, J. C., Markus, T., Boisvert, L., Miller, J. and Barrett, A.: Changes in Arctic  
672 melt season and implications for sea ice loss, *Geophys Res Lett*, 41(4),  
673 2013GL058951, doi:10.1002/2013GL058951, 2014.
- 674 Stroeve, J. C., Serreze, M. C., Holland, M. M., Kay, J. E., Malanik, J. and Barrett, A.  
675 P.: The Arctic's rapidly shrinking sea ice cover: a research synthesis, *Climatic*  
676 *Change*, 110, 1005-1027, 2012.
- 677 Stuiver, M., Reimer, P.J., and Reimer, R.W.: CALIB 7.1 [WWW program] at  
678 <http://calib.org>, 2010.
- 679 SWERUS C3 2014 Expedition. The Swedish –Russian – US Arctic Ocean  
680 Investigation of Climate-Cryosphere-Carbon Interactions – The SWERUS-C3 2014  
681 Expedition Cruise Report Leg 2 (of 2)  
682 (<ftp://ftp.geo.su.se/martinj/outgoing/SWERUSC3/Leg2%20Cruise%20Report/>).
- 683 Taldenkova, E., Bauch, H. A., Stepanova, A., Ovsepyan, Y., Pogodina, I.,  
684 Klyuvitkina, T., and Nikolaev, S.: Benthic and planktic community changes at the  
685 North Siberian margin in response to Atlantic water mass variability since last  
686 deglacial times, *Mar Micropaleontol*, 96-97, 13-28,  
687 doi:10.1016/j.marmicro.2012.06.007, 2012.
- 688 Taldenkova, E., Bauch, H.A., Stepanova, A., Strezh, A., Dem'yankov, S.,  
689 Ovsepyan, Ya., Postglacial to Holocene benthic assemblages from the Laptev  
690 Sea: paleoenvironmental implications, *Quaternary International*, 183, 40–60, 2008.
- 691 Taldenkova, E., Bauch, H. A., Stepanova, A., Dem'yankov, S. and Ovsepyan, A.:  
692 Last postglacial environmental evolution of the Laptev Sea shelf as reflected in  
693 molluscan, ostracodal, and foraminiferal faunas, *Global Planet Change*, 48, 223-  
694 251, 2005.



- 695 Wassmann, P., Duarte, C. M., Agusti, S., and Sejr, M. K.: Footprints of climate  
696 change in the Arctic marine ecosystem, *Global Change Biol*, 17, 1235-1249, 2011.
- 697 Whatley, R., Eynon, M. and Mogueilevsky, A.: The depth distribution of Ostracoda  
698 from the Greenland Sea, *Journal of Micropalaeontology*, 17, 15–32, 1998.
- 699 Whatley, R. C., Eynon, M. P. and Mogueilevsky, A.: Recent Ostracoda of the  
700 Scoresby Sund Fjord system, East Greenland, *Revista Española de*  
701 *Micropaleontología*, 28(2), 5-23, 1996.
- 702 Wollenburg, J. E., Kuhnt, W., and Mackensen, A.: Changes in Arctic Ocean  
703 paleoproductivity and hydrography during the last 145 kyr: The benthic  
704 foraminiferal record, *Paleoceanography*, 16, 65-77, 2001.
- 705 Xiao, X., Stein, R., Fahl, K.: MIS 3 to MIS 1 temporal and LGM spatial variability in  
706 Arctic Ocean sea ice cover: Reconstruction from biomarkers, *Paleoceanography*,  
707 30, doi:10.1002/2015PA002814, 2015.
- 708 Yasuhara, M., Stepanova, A., Okahashi, H., Cronin, T.M. and Brouwers, E.M.:  
709 Taxonomic revision of deep-sea Ostracoda from the Arctic Ocean,  
710 *Micropaleontology*, 60, 399-444, 2014.
- 711 Zirikian, C. A. A., Stepanova, A. Y., and Grutzner, J.: Glacial-interglacial variability  
712 in deep sea ostracod assemblage composition at IODP Site U1314 in the subpolar  
713 North Atlantic, *Mar Geol*, 258, 69-87, 2009.
- 714 Zemp, M., Frey, H., Gartner-Roer, I., Nussbaumer, S. U., Hoelzle, M., Paul, F.,  
715 Haeberli, W., Denzinger, F., Ahlstrom, A. P., Anderson, B., Bajracharya, S.,  
716 Baroni, C., Braun, L. N., Caceres, B. E., Casassa, G., Cobos, G., Davila, L. R.,  
717 Granados, H. D., Demuth, M. N., Espizua, L., Fischer, A., Fujita, K., Gadek, B.,  
718 Ghazanfar, A., Hagen, J. O., Holmlund, P., Karimi, N., Li, Z. Q., Pelto, M., Pitte, P.,  
719 Popovnin, V. V., Portocarrero, C. A., Prinz, R., Sangewar, C. V., Severskiy, I.,  
720 Sigurosson, O., Soruco, A., Usabaliev, R., Vincent, C., and Correspondents, W.  
721 N.: Historically unprecedented global glacier decline in the early 21st century, *J*  
722 *Glaciol*, 61, 745-+, 2015.



Table 1. Expedition and core site data for cores presented in this study.

| Year | Expedition      | Core name         | Latitude | Longitude | Water depth (m) | Location              |
|------|-----------------|-------------------|----------|-----------|-----------------|-----------------------|
| 2014 | SWERUS-L2       | SWERUS-L2-32-MC4  | 85.14    | 151.59    | 837             | Lomonosov Ridge       |
| 2014 | SWERUS-L2       | SWERUS-L2-32-GC2  | 85.15    | 151.66    | 828             | Lomonosov Ridge       |
| 2014 | SWERUS-L2       | SWERUS-L2-24-MC4  | 78.80    | 165.38    | 982             | E. Siberian Sea Slope |
| 2014 | SWERUS-L2       | SWERUS-L2-28-MC1  | 79.92    | 154.35    | 1145            | E. Siberian Sea Slope |
| 2014 | SWERUS-L2       | SWERUS-L2-33-TWC1 | 84.28    | 148.65    | 888             | Lomonosov Ridge       |
| 2014 | SWERUS-L2       | SWERUS-L2-34-MC4  | 84.28    | 148.71    | 886             | Lomonosov Ridge       |
| 1994 | AOS SR96-1994   | PI-94-AR-BC28     | 88.87    | 140.18    | 1990            | Lomonosov Ridge       |
| 1991 | Arctic 91       | PS 2179-3 MC      | 87.75    | 138.16    | 1228            | Lomonosov Ridge       |
| 1991 | Arctic 91       | PS 2185-4 MC      | 87.53    | 144.48    | 1051            | Lomonosov Ridge       |
| 1994 | AOS SR96-1994   | PI-94-AR-BC8      | 78.13    | 176.75    | 1031            | Mendelev Ridge        |
| 1994 | AOS SR96-1994   | PI-94-AR-BC12A    | 79.99    | 174.29    | 1683            | Mendelev Ridge        |
| 2005 | HOTRAX          | HLY0503-6         | 78.29    | -176.99   | 800             | Mendelev Ridge        |
| 1994 | AOS SR96-1994   | P1-94-AR-PC10     | 78.15    | -174.63   | 1673            | Mendelev Ridge        |
| 1992 | USGS-Polar Star | P1-92-AR P40      | 76.26    | -157.55   | 700             | Northwind Ridge       |
| 1992 | USGS-Polar Star | P1-92-AR-P30      | 75.31    | -158.05   | 765             | Northwind Ridge       |
| 2007 | LOMROG 07       | LOMROG07-PC-04    | 86.70    | -53.77    | 811             | Lomonosov Ridge       |
| 1996 | Oden 96         | 96-12-1PC         | 87.10    | 144.77    | 1003            | Lomonosov Ridge       |

Table 2. Radiocarbon dates for SWERUS 32 cores, uncalibrated  $^{14}\text{C}$  age and calibrated  $^{14}\text{C}$  chronology.

| 32-MC/GC chronology                           |            |                     |       |       | Unmodelled |                     | Modelled |        |       |
|---|------------|---------------------|-------|-------|------------|---------------------|----------|--------|-------|
| Lab number ( $^{14}\text{C}$ date age, error) | Depth (cm) | 2 sigma (2 std dev) |       | mean  | error      | 2 sigma (2 std dev) |          | mean** | error |
|   |            | from                | to    |       |            | from                | to       |        |       |
| OS-124799 (3410, 25)                          | 2.5        | 3168                | 2698  | 2912  | 124        | 3045                | 2605     | 2802   | 105   |
| OS-124798 (6110, 20)                          | 4.5        | 6435                | 5974  | 6213  | 116        | 6317                | 5902     | 6140   | 113   |
| OS-124599 (7920, 35)                          | 5.5        | 8313                | 7874  | 8085  | 110        | 8176                | 7766     | 7972   | 101   |
| OS-124598 (8290, 30)                          | 8.5        | 8715                | 8207  | 8465  | 119        | 8576                | 8187     | 8385   | 99    |
| OS-124597 (11000, 35)                         | 11.5       | 12525               | 11661 | 12094 | 222        | 12191               | 11353    | 11831  | 230   |



|                            |      |       |       |       |      |       |       |       |      |
|----------------------------|------|-------|-------|-------|------|-------|-------|-------|------|
| OS-124754<br>(11200, 40)   | 14.5 | 12635 | 12040 | 12365 | 164  | 12625 | 12008 | 12381 | 165  |
| OS-125185<br>(18650, 80)   | 19.5 | 22116 | 21357 | 21729 | 183  | 21973 | 21252 | 21637 | 179  |
| OS-125190<br>(29400, 280)  | 24.5 | 33567 | 31805 | 32733 | 462  | 33298 | 31585 | 32423 | 455  |
| OS-125192<br>(35400, 560)  | 31.5 | 40705 | 38099 | 39301 | 638  | 40858 | 38451 | 39608 | 608  |
| OS-127484<br>(40000, 1700) | 33*  | 47589 | 40881 | 43837 | 1646 | 44472 | 40403 | 42428 | 1002 |

All ages as calibrated years BP

$\Delta R = 300 \pm 100$  years (Reimer and Reimer, 2001)

Marine13 calibration curve (Reimer et al., 2013)

\*Sample collected from 32-GC, original depth was 36 cm but corrected by 3 cm based on ostracode correlation with 32-MC

\*\*We used the modeled, mean, 2-sigma age to plot species' relative frequencies.

Table 3. List of species included in genus-level groups.

| Group name                | Species included in Group:  |
|---------------------------|---|
| <i>Cytheropteron</i> spp. | <i>Cytheropteron higashikawai</i> Ishizaki 1981, <i>Cytheropteron scoresbyi</i> Whatley and Eynon 1996, <i>Cytheropteron sedovi</i> Schneider 1969 and <i>Cytheropteron parahamatsum</i> Yasuhara, Stepanova, Okahashi, Cronin and Brouwers 2014.   |
| <i>Polycopse</i> spp.     | <i>P. inornata</i> Joy & Clark, 1977 and <i>P. bireticulata</i> Joy & Clark, 1977. (For scanning electron microscope images, see Joy & Clark 1977: Plate 3, Fig. 1; Yasuhara et al., 2014: Plate 3, Figs 2-5 and Plate 2, Figs 1-2.)<br>May include: <i>P. arcys</i> (Joy & Clark, 1977), <i>P. punctata</i> (Sars 1869), <i>P. bispinosa</i> Joy & Clark 1977, <i>P. horrida</i> Joy & Clark 1977, <i>P. moenia</i> Joy & Clark 1977, <i>P. semipunctata</i> Joy & Clark 1977, <i>P. obicularis</i> Sars 1866. <i>P. pseudoinornata</i> Chavtur, 1983 and <i>P. reticulata</i> Muller 1894 |



Table 4. Summary of indicator species, pertinent aspects of their modern ecology and paleoenvironmental significance.

| Species  | Modern ecology / paleoenvironmental significance  |
|--|---|
| <i>Acetabulastoma arcticum</i> (Schornikov, 1970). | The stratigraphic distribution of <i>A. arcticum</i> is used as an indicator of periods when the Arctic Ocean experienced thicker sea-ice conditions. This pelagic ostracode is a parasite on <i>Gammarus</i> amphipods that live under sea ice in modern, perennially sea-ice-covered regions in the Arctic (Schornikov, 1970). Cronin et al. (2010) used <i>A. arcticum</i> 's presence in 49 late Quaternary Arctic sediment cores as a proxy to reconstruct the Arctic Ocean's sea-ice history during the last ~45 ka.  |
| <i>Krithe</i> spp.                                 | Species of the genus <i>Krithe</i> typically occur in low-nutrient habitats spanning across a range of cold, interstadial temperatures but are especially characteristic of AODW (Cronin et al., 1994; 1995; 2014). In SWERUS-32 cores, <i>K. huntii</i> was far more prevalent than <i>K. minima</i> . From a modern depth-distribution analysis using AOD, <i>K. huntii</i> appears in greatest abundance (50-80% of the assemblage) at depths between 2000-4400 m, however, this taxon is also found in significant numbers (20-50%) at depths between 400-2000 m. With a preference for deeper, cold, well-ventilated depths, <i>Krithe</i> spp. events are useful in identifying late Quaternary shifts in Arctic Ocean water masses and making biostratigraphic correlations (Cronin et al., 2014). |
| <i>Polycope</i> spp.                               | Today, this Atlantic-derived genus is in highest abundance (40-60% of assemblage) in cold intermediate-depth waters between 800-2300 mwd. It characterizes fine-grained, organic rich sediment in well-oxygenated water. In fossil assemblages, <i>Polycope</i> is indicative of areas with high productivity that are seasonally ice-free or have variable or thin sea-ice cover (Cronin et al., 1995; Poirier et al., 2012).  |
| <i>Cytheropteron</i> spp.                          | The two dominant <i>Cytheropteron</i> species in 32-MC and 32-GC are <i>C. sedovi</i> and <i>C. scoresbyi</i> , along with lower but significant numbers of <i>C. parahamatum</i> (reaches 24% of assemblage at 10 ka) and <i>C. higashikawai</i> (fluctuates in very low numbers between 0-3% at any given time in downcore samples). These particular <i>Cytheropteron</i> species are broadly diagnostic of deeper, well-ventilated water masses (AIW and AODW).   |
| <i>Pseudocythere caudata</i> Sars 1866             | This species of N. Atlantic origin rarely exceeds >15% in modern Arctic Ocean assemblages. It characterizes lower AW and AI water at depths of 1000-2500 m and usually co-occurs with <i>Polycope</i> spp. in fossil assemblages. (Cronin et al., 1994, 1995).  |

Table 5. Although *R. mirabilis* (Brady, 1868) is known and named from Pleistocene sediments in England and Scotland (Brady et al., 1874), this list cites various workers since that have documented this species in Arctic deposits dating back to the late Pliocene, when summer bottom temperatures were inferred to be up to 4°C warmer than today.

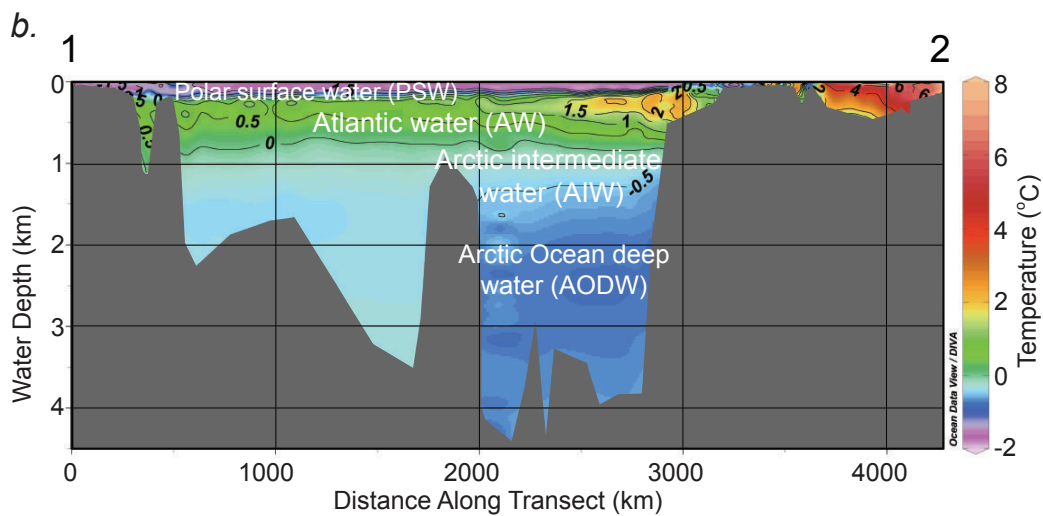
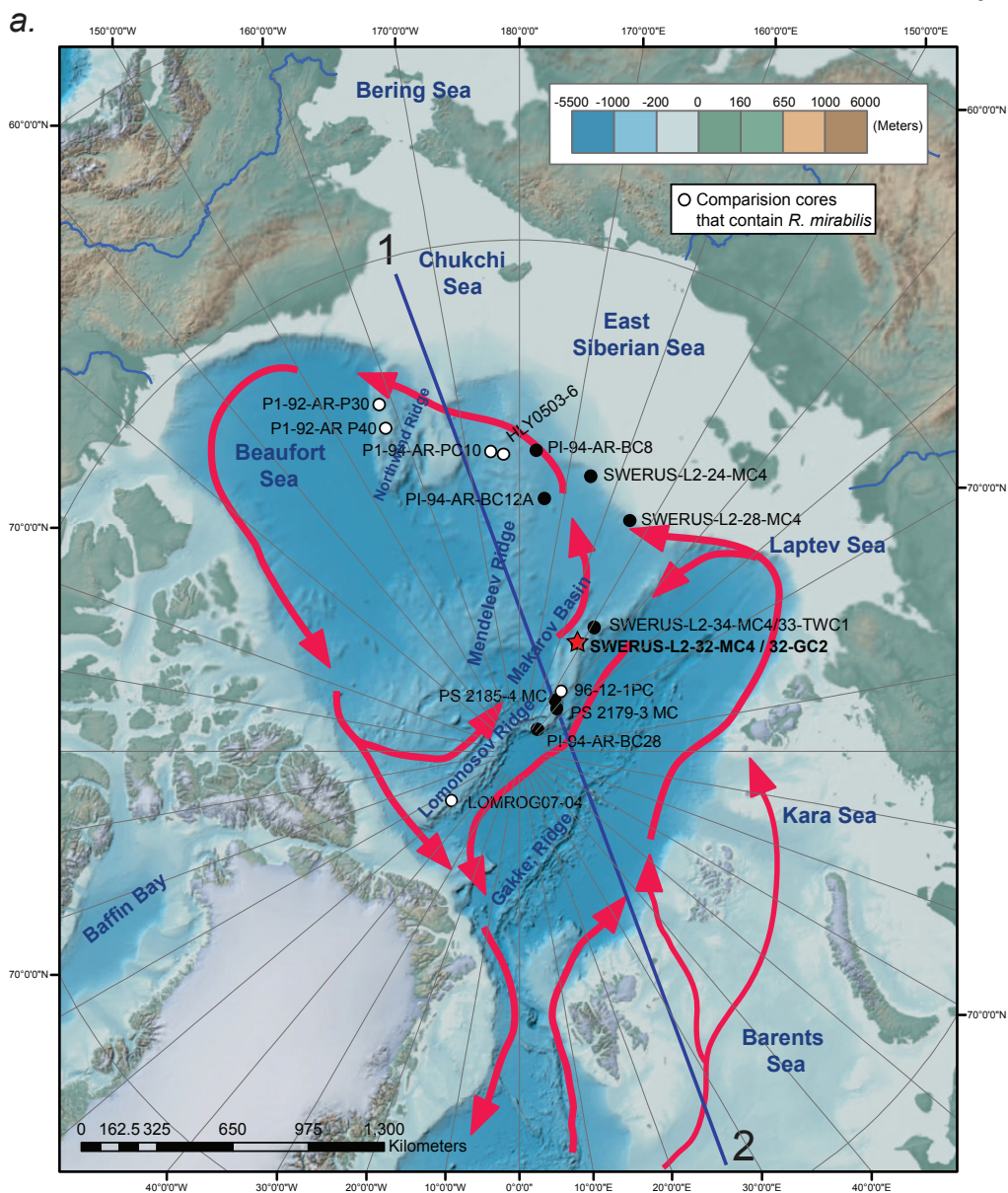
| Citation                | Location / Formation (Age)                                      |
|-------------------------|---|
| Siddiqui (1988)         | Eastern Beaufort Sea's Iperk sequence (Plio-Pleistocene)        |
| Repenning et al. (1987) | Alaska's North Slope Gubik Formation (Pliocene)                 |
| Penney (1990)           | Central North Sea deposits (early Pleistocene age, 1.0-0.73 Ma) |
| Feyling-Hassen (1990)   | East Greenland's Kap København Formation (late Pliocene)        |
| Penney (1993)           | East Greenland's Lodin Elv Formation (late Pliocene)            |



Figures 1-7



Fig. 1



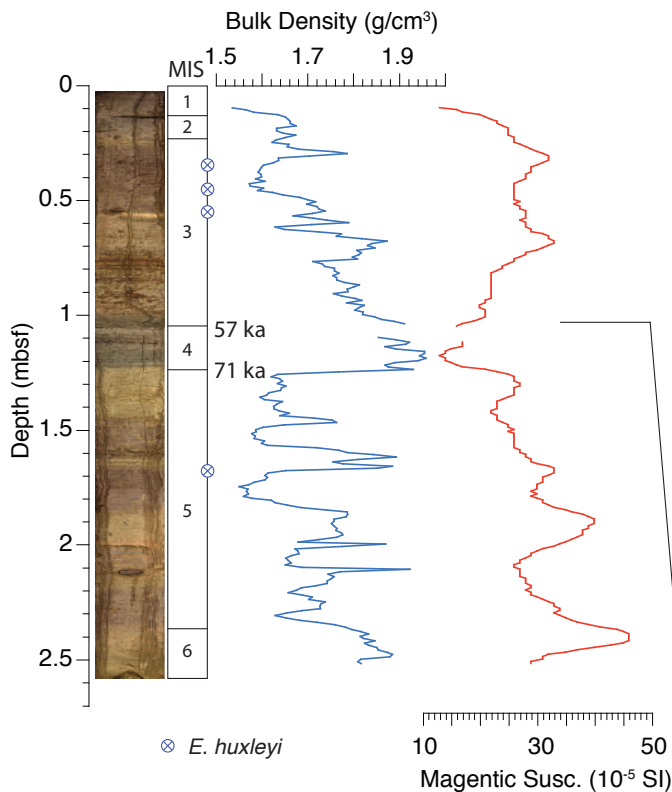


Fig. 2

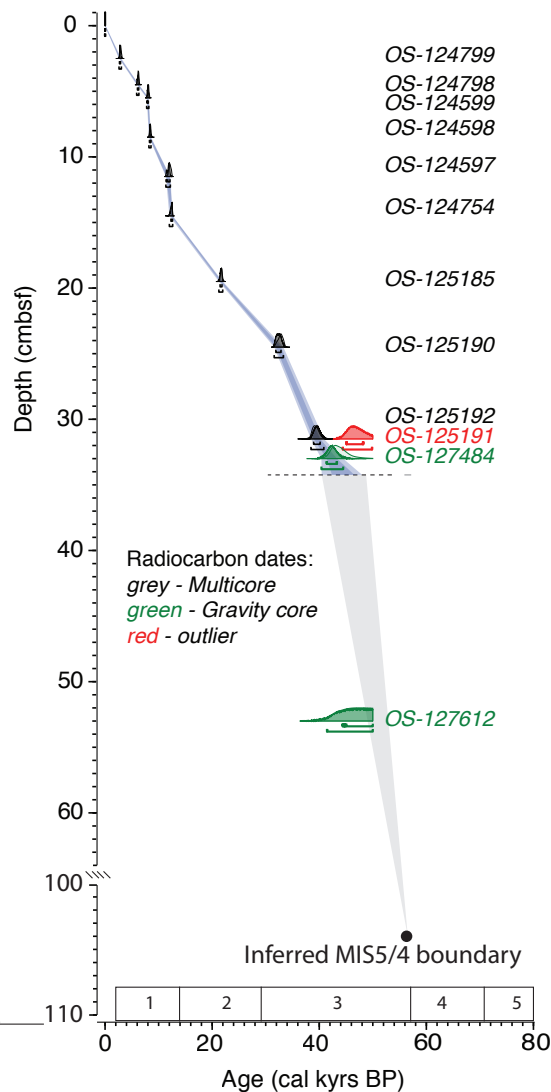




Fig. 3

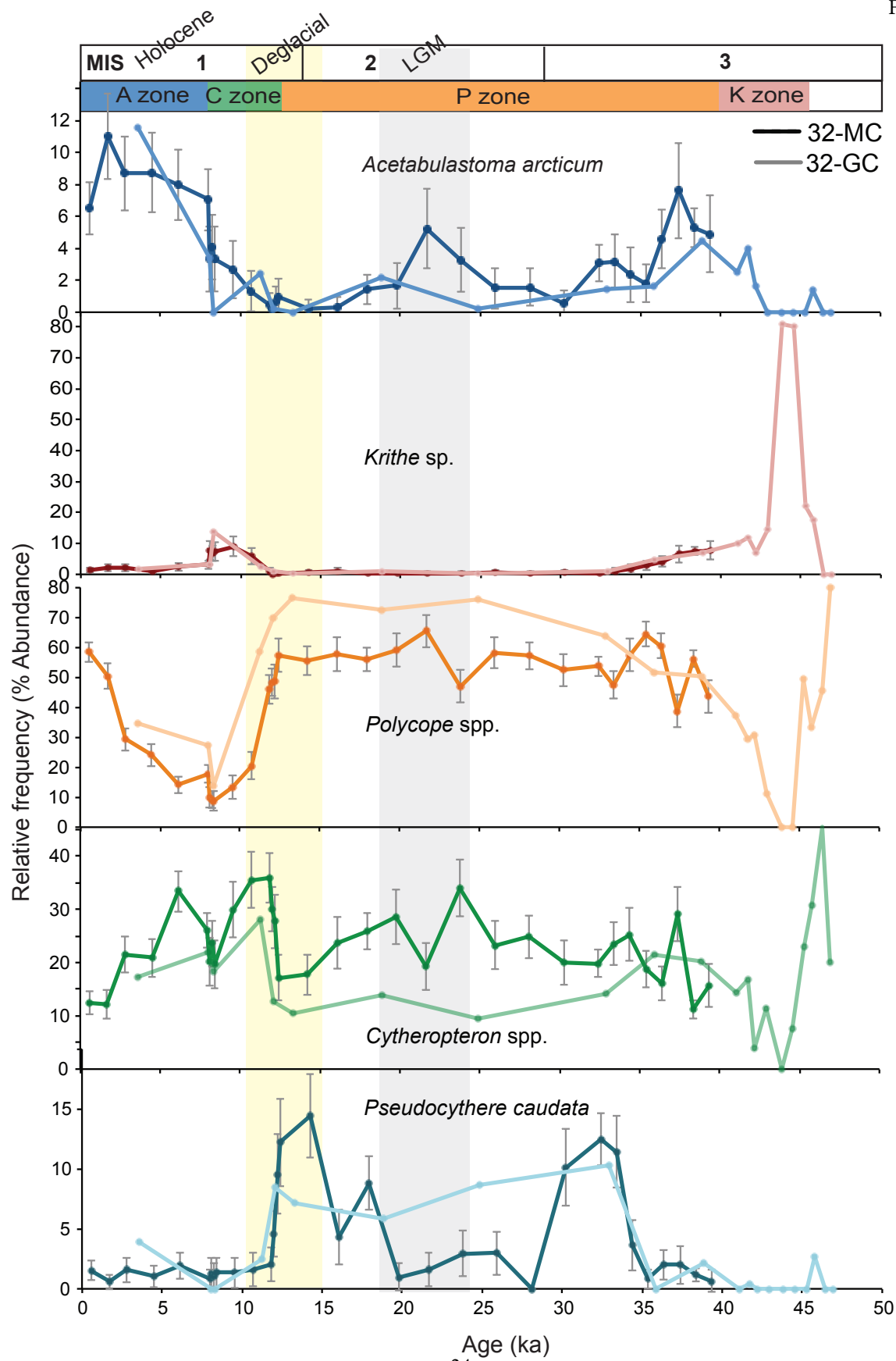




Fig. 4

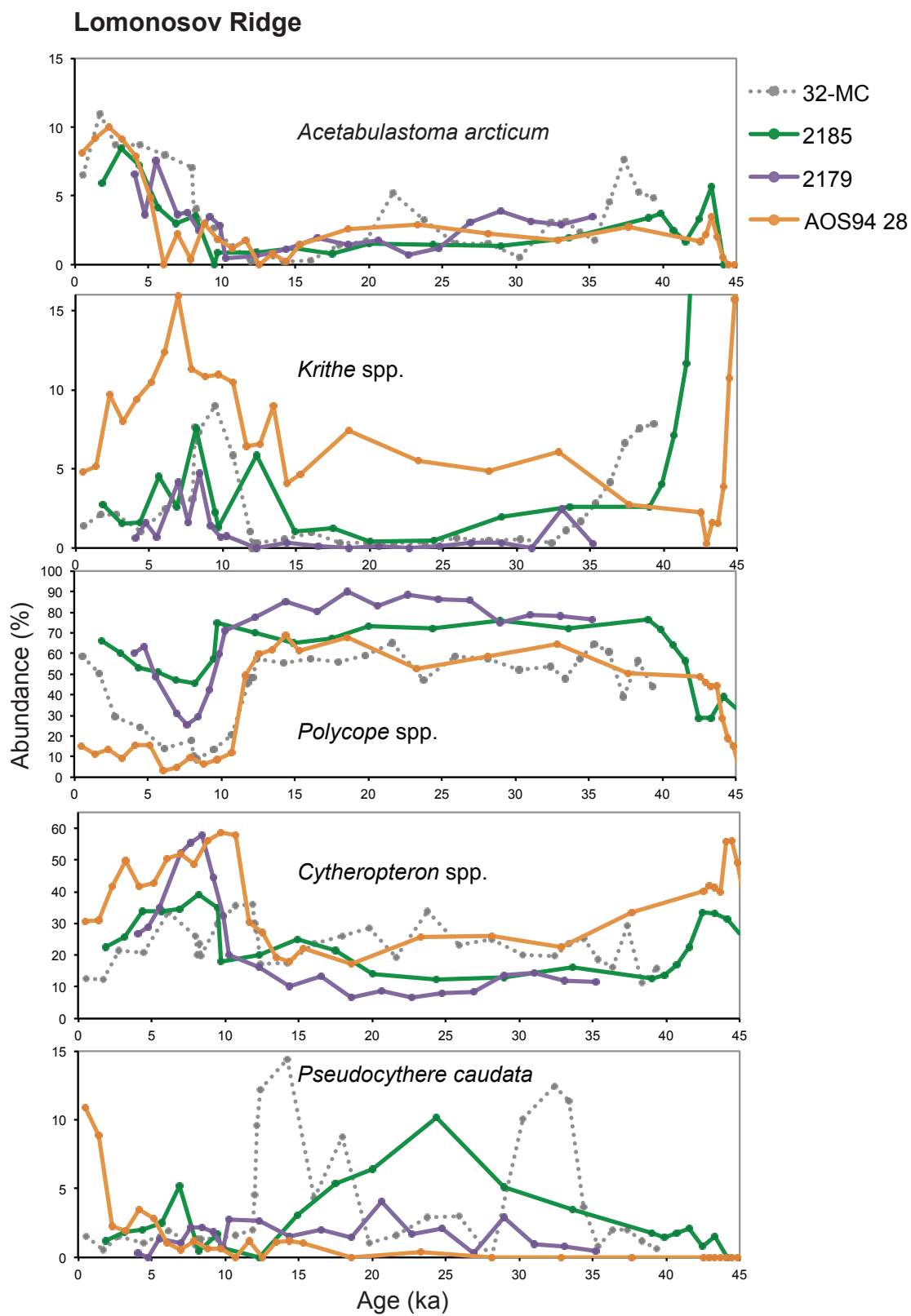




Fig. 5

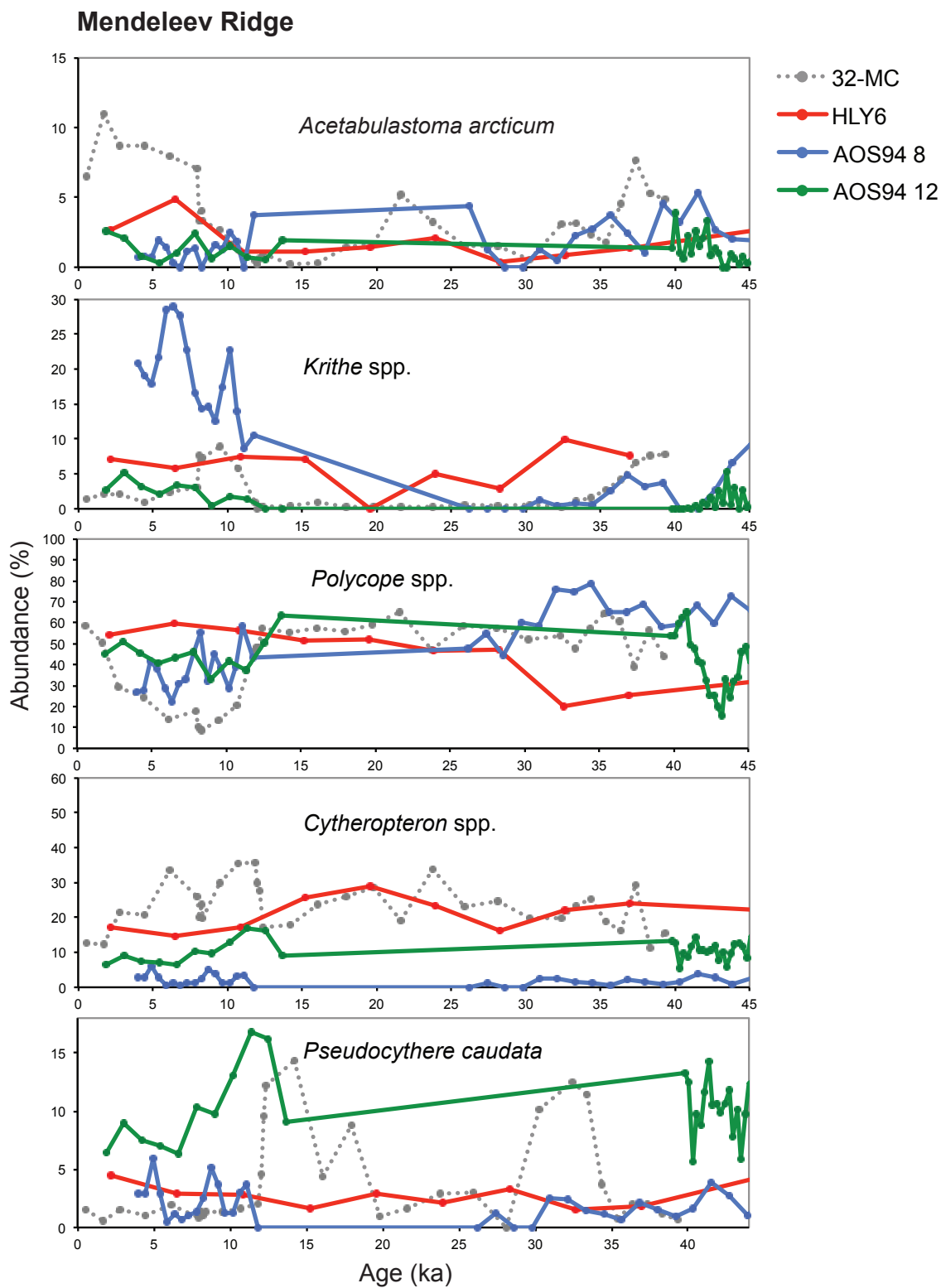




Fig. 6

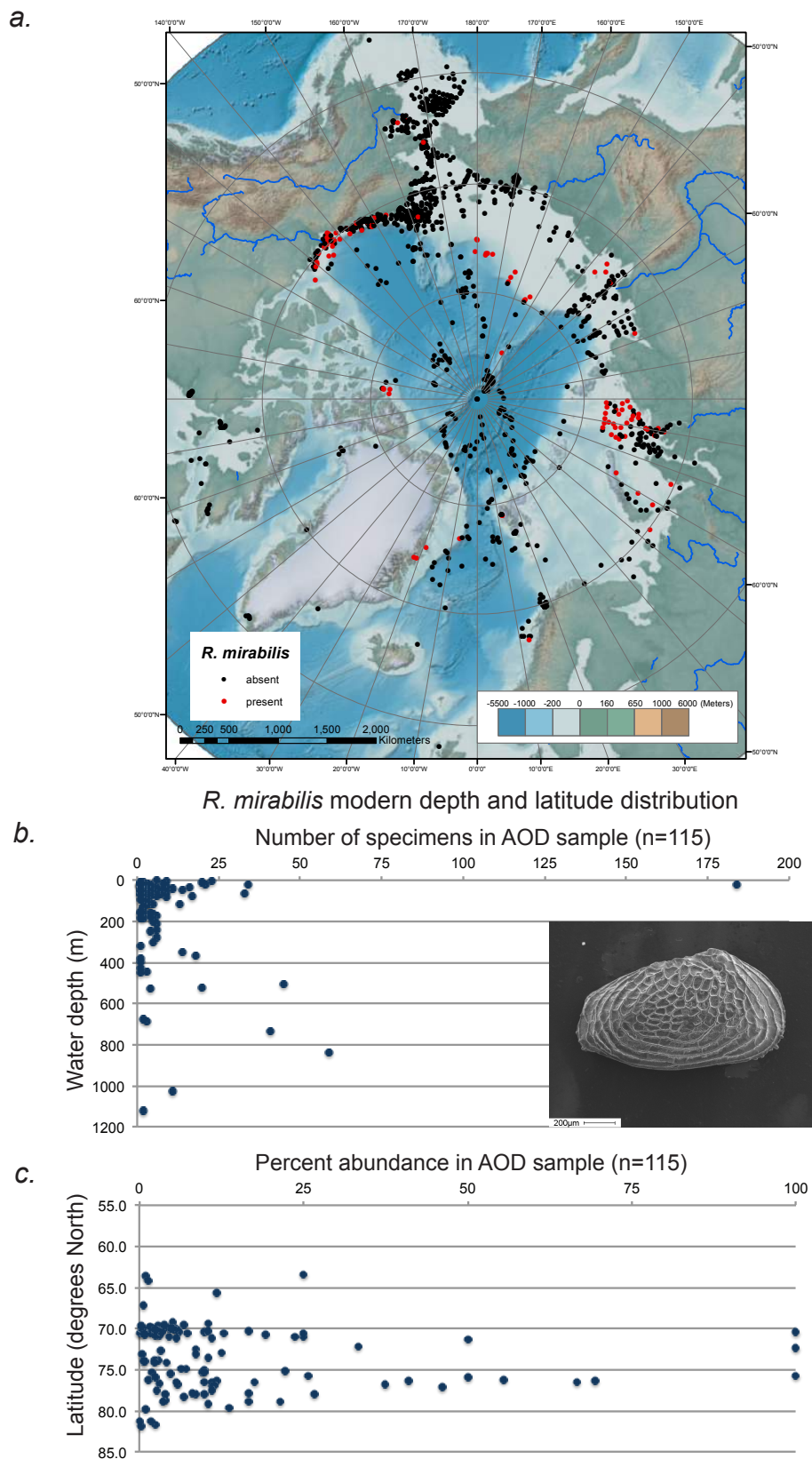




Fig. 7

